



A comprehensive study of Bardeen stars with conformal motion in $f(\mathcal{G})$ gravity

Aisha Rashid^{1,a}, Adnan Malik^{2,3,b}, M. Farasat Shamir^{4,c}

¹ National University of Computer and Emerging Sciences, Lahore Campus, Lahore, Pakistan

² School of Mathematical Sciences, Zhejiang Normal University, Jinhua, Zhejiang, China

³ Department of Mathematics, University of Management and Technology, Sialkot Campus, Lahore, Pakistan

⁴ School of Mathematical Sciences, Queen Mary University of London, London, UK

Received: 17 August 2023 / Accepted: 13 October 2023
© The Author(s) 2023

Abstract In this manuscript, we use the conformal killing vectors to solve the Einstein–Maxwell field equations in the background of modified $f(\mathcal{G})$ gravity. We consider the observational data for four different stars namely *PSR J1614 – 2230*, *PSR J1930 + 327*, *Cen X – 3* and *Vela X – 1* respectively. By using the data, we derive the physical parameters from the matching criteria using conformal killing vectors and the exterior Bardeen geometry. Furthermore, several physical properties of compact stellar structures are examined in order to achieve the physical validity and stability for considered models. The graphical analysis including energy density, pressure components, equation of state parameters, and energy conditions are examined. Moreover, the equilibrium conditions through Tolman–Oppenheimer–Volkoff equation and stability criteria through adiabatic index for the charged stellar structure study are investigated. It is worth noting that all of these compact objects are physically viable and stable under conformal motion in context of Bardeen geometry for two different models of $f(\mathcal{G})$ theory of gravity. Conclusively, the results show that $f(\mathcal{G})$ gravity with Bardeen model may provide more massive stellar objects as compared to general relativity.

1 Introduction

Although general relativity (*GR*) is a fantastic, well-established, and extremely significant theory, several worthwhile improvements have been suggested by academics over the past cen-

tury. Some of these gravitational theories include $f(\mathcal{R})$ [1–5], $f(\mathcal{R}, \mathcal{G})$ [6,7], $f(\mathcal{G})$ [8], $f(\mathcal{R}, T)$ [9,10], $f(\mathcal{Q})$ [11], $f(\mathcal{R}, \phi)$ [12,13] and $f(\mathcal{R}, \phi, X)$ [14,15] modified theories of gravity. These theories involve modifications to classical GR to better understand accelerating universe and to explore scenarios, where GR may provide an insufficient explanation. It has led to a search for modified or extended gravitational theories capable of addressing such challenges. Cosmology has identified two unexplained components, dark matter (DM) and dark energy (DE), which are responsible for the universe's accelerating expansion. It is assumed that these modified theories of gravity give better explain the issues of DM and DE [16–23]. Furthermore, these modified theories of gravities are also very helpful for the investigation of stellar structures. Mak and Harko [24] discussed the exact analytical solution describing the interior of a charged strange quark star under the assumption of spherical symmetry and the existence of a one-parameter group of conformal motions. Chaisi and Maharaj [25] investigated the exact interior solutions to the Einstein field equations for anisotropic spheres and utilized a procedure that necessitates a choice for the energy density and the radial pressure. Kalam et al. [26] proposed a de-Sitter model for an anisotropic strange star with the Krori–Barua spacetime and incorporated the existence of the cosmological constant on a small scale to study the structure of anisotropic strange stars.

Modified $f(\mathcal{G})$ theory of gravity has been very attractive among the researcher for the discussion of stellar structures. Ilyas [27] investigated some of the interior configuration of static anisotropic spherical stellar charged structures in the regime of $f(\mathcal{G})$ gravity, and analyzed the solution with the help of Krori–Barua technique. Felice and Tsujikawa [28] presented a number of explicit $f(\mathcal{G})$ models in which a cosmic acceleration is followed by the matter era.

^a e-mail: aisharashid987@gmail.com

^b e-mails: adnan.malik@zjnu.edu.cn; adnan.malik@skt.utm.edu.pk; adnanmalik_chheena@yahoo.com (corresponding author)

^c e-mails: f.shamir@qmul.ac.uk; farasat.shamir@gmail.com

Naz and Shamir [29] investigated the dynamical behavior of stellar structures in $f(\mathcal{G})$ theory of gravity by using Tolman-Kuchowicz spacetime. Shamir and Naz [30] explored some relativistic configurations of stellar objects for static spherically symmetric structures in the context of modified $f(\mathcal{G})$ gravity, and developed the equations of motion for spherically symmetric spacetime in the presence of anisotropic matter distribution. The same authors [31] investigated some possible emergence of relativistic compact stellar objects in modified $f(\mathcal{G})$ gravity using Noether symmetry approach and constructed Noether symmetry generators along with associated conserved quantities by considering the standard choice of viable $f(\mathcal{G})$ gravity model. Malik et al. [32] investigated the anisotropic stellar structures using Bardeen geometry in Modified $f(\mathcal{G})$ theory of gravity.

Symmetries can play an important role to investigate the natural relation between geometry and matter through the Einstein's equations. Among the well known symmetries, conformal killing vector (CKV) can provide some better results as they provide a deeper insight into the spacetime geometry. Herrera et al. [33–35] were among the pioneers who gave the general treatment of the spheres admitting a one parameter group of conformal motions. Maartens and Maharaj [36] investigated the solutions of the Einstein–Maxwell equations for static spheres of charged imperfect fluids, where the space-time geometry was assumed to admit a conformal symmetry. Bhar et al. [37] provided a new class of interior solutions for anisotropic stars admitting conformal motion in higher-dimensional noncommutative space-time. Usmani et al. [38] proposed a new model of a gravastar admitting conformal motion, which was assumed to be internally charged, with an exterior defined by a Reissner–Nordstrom instead of a Schwarzschild line element. Das et al. [39] provided a set of exact spherically symmetric solutions describing the interior of a relativistic star under $f(T)$ modified gravity and studied several cases of interest to explore physically valid features of the solutions. Zubair et al. [40] discussed the interior solutions of fluid sphere in $f(R, T)$ gravity admitting CKV.

Equation of state (EoS) is extremely useful for studying the equilibrium structures of a compact objects within the context of *GR*. Researchers have worked on the topic of physical properties of strange quark configurations utilizing the EoS specifically MIT bag model in recent years. A quark bag model with an appropriate EoS was used to calculate the accelerating expansion of the early universe [32]. Deb et al. [41] attempted to find a singularity free solution of Einstein's field equations for compact stellar objects by using MIT bag model, and considering Schwarzschild metric as the exterior spacetime. Coley and Tupper [42] studies the perfect fluid spherically symmetric spacetimes admitting a proper inheriting CKV. Abbas and Shahzad [43] studied a new solution for an isotropic compact star model admitting confor-

mal motion in the background of Rastall theory and several physical aspects of the model were explored analytically to observe the behavior of compact stars. Jape et al. [44] generated a new generalized regular charged anisotropic exact model that admitted conformal symmetry in static spherically symmetric spacetime and that model was examined for physical acceptability as a realistic stellar model.

In the preceding framework, we are primarily interested in studying the evolution of compact stellar objects accepting *CKV* utilizing two distinct models of $f(\mathcal{G})$ theory of gravity. This work is the continuation of a recently reported investigation in which Shamir and Rashid [45] studied the stellar structures in $f(R)$ modified theory of gravity admitting conformal motion. We specifically extend this approach to investigate the dynamical behaviour of compact sphere in modified $f(\mathcal{G})$ gravity. Moreover, we use Bardeen geometry as an exterior space-time and presume the isotropic matter for our current analysis. The organization of this paper is as follows: Sect. 2 presents a basic formulation of modified $f(\mathcal{G})$ gravity with an isotropic matter distribution, including a detailed discussion of *CKV*. Moving on to Sect. 3, we use the modified field equations to obtain the expressions for physical quantities like energy density and pressure for two different $f(\mathcal{G})$ gravity models. Section 4 employs matching conditions to determine the values of physical parameters. In Sect. 5, a thorough analysis of the physical characteristics is conducted. Finally, in Sect. 6, we provide a comprehensive discussion of our key findings.

2 Gauss–Bonnet gravity and Einstein–Maxwell field equation

In current section, we present details of equation of motion of Gauss Bonnet $f(\mathcal{G})$ gravity in presences of charge. The modified Einstein–Hilbert action with charge is given as

$$S = \int d^4x \sqrt{-g} \left[\frac{R}{2\kappa} + f(\mathcal{G}) \right] + L_e + L_m, \quad (1)$$

where, f is the function of Gauss Bonnet invariant \mathcal{G} , the Lagrangian is represented by L_m , g is the determinant of metric tensor $g_{\mu\nu}$ and the lagrangian of electromagnetic field is denoted by L_e . We have the following expression of \mathcal{G} and L_e

$$\mathcal{G} = R^2 - 4R_{\alpha\beta}R^{\alpha\beta} + R_{\alpha\beta\mu\nu}R^{\alpha\beta\mu\nu}, \quad (2)$$

$$L_e = \frac{1}{16\pi} F_{\xi\eta} F_{\alpha\beta} g^{\xi\alpha} g^{\eta\beta}. \quad (3)$$

In Eq. (2) R , $R_{\alpha\beta}$ and $R_{\alpha\beta\mu\nu}$ are Ricci scalar, Ricci tensor and Riemannian tensors. In Eq. (3) $F_{\xi\eta}$ represents an electromagnetic field tensor along with electromagnetic four potential vector A_ξ given as

$$F^{\xi\eta} = A_{\xi,\eta} - A_{\eta,\xi}. \quad (4)$$

The Einstein Maxwell Field Equations (EMFE) are given by the following expression

$$F_{;\eta}^{\xi\eta} = -4\pi j^\xi. \quad (5)$$

There is single non-vanishing element of *EMFE* i.e. F^{01} , and obtained with the help of Eqs. (4) and (5)

$$F^{01} = \frac{q}{r^2} e^{-\frac{\chi+\lambda}{2}}, \quad (6)$$

where, q exhibit total charge

$$q = 4\pi \int 4\sigma \omega^2 e^{-\frac{\lambda}{2}} d\omega. \quad (7)$$

Moreover, we get the electric intensity E as

$$E = -F^{01} F_{01} = \frac{q}{r^2}. \quad (8)$$

In Eq. (5), $j^\xi = \sigma v^\xi$ is called electromagnetic four current vector along with the charge density σ . The following form of space-time is considered

$$ds^2 = -(e^\lambda dr^2 + r^2 d\theta^2 + r^2 \sin^2 \theta d\phi^2) + e^\chi dt^2. \quad (9)$$

The energy momentum tensor in presences of charge is given by

$$T_{\chi\xi} = (\rho + p)u_\chi u_\xi - pg_{\chi\xi} - \frac{1}{4\pi} \left(g_{\xi\beta} F^{\alpha\beta} F_{\xi\alpha} - \frac{1}{4} g_{\chi\xi} F_{\alpha\psi} F^{\alpha\psi} \right). \quad (10)$$

The ρ and p are energy density and pressure in Eq. (10) respectively. The velocity four vectors are satisfying the following conditions

$$u^\chi u_\chi = 1, v^\chi v_\chi = -1. \quad (11)$$

The modified field equations of $f(\mathcal{G})$ gravity are as follows

$$G^{eff}_{\chi\xi} = \kappa T_{\chi\xi}^{eff}, \quad (12)$$

where, $T_{\chi\xi}^{eff}$ is the effective energy momentum tensor given as

$$T_{\chi\xi}^{eff} = T_{\chi\xi} + E_{\chi\xi} - \frac{8}{\kappa} \left[R_{\chi\alpha\xi\beta} + R_{\alpha} g_{\beta\chi} - R_{\alpha\beta} g_{\xi\chi} - R_{\chi\xi} g_{\alpha\beta} + R_{\chi\beta} g_{\xi\alpha} + \frac{R}{2} (g_{\chi\xi} g_{\alpha\beta} - g_{\chi\beta} g_{\xi\alpha}) \right] \nabla^\alpha \nabla^\beta f_{\mathcal{G}} - (\mathcal{G} f_{\mathcal{G}} - f) g_{\chi\xi}. \quad (13)$$

All the aforementioned information is utilized to derive the field equations presented as

$$\begin{aligned} \rho^{eff} + E^2 &= \rho - 8e^{-2\lambda} (\mathcal{G} f_{\mathcal{G}} \mathcal{G}'^2 + f_{\mathcal{G}} \mathcal{G}'') \left(\frac{e^\lambda - 1}{r^2} \right) \\ &+ 4e^{-2\lambda} \lambda' \mathcal{G}' f_{\mathcal{G}} \left(\frac{e^\lambda - 3}{r^2} \right) - (\mathcal{G} f_{\mathcal{G}} - f), \end{aligned}$$

$$p^{eff} - E^2 = p - 4e^{-2\lambda} \lambda' \mathcal{G}' f_{\mathcal{G}} \left(\frac{e^\lambda - 3}{r^2} \right) \quad (14)$$

$$+ (\mathcal{G} f_{\mathcal{G}} - f), \quad (15)$$

$$\sigma = \frac{e^{-\frac{\lambda}{2}}}{4\pi r^2} (r^2 E)'. \quad (16)$$

Furthermore, in order to examine the intrinsic structure of compact stars, we use the MIT bag model [47] that illustrates relation between p and ρ in interior of the sphere given as,

$$p = \frac{1}{3}(\rho - 4B). \quad (17)$$

In above equation, B is the bag constant. Based on the previously provided information, the E^2 is given by the following expression

$$\begin{aligned} E^2 = -\frac{e^{-\lambda(r)}}{4r^2} &\left(4Br^2 e^{\lambda(r)} + 2r^2 f(\mathcal{G}) e^{\lambda(r)} - 2\mathcal{G}r^2 f_{\mathcal{G}} e^{\lambda(r)} \right. \\ &+ 8f_{\mathcal{G}} \mathcal{G}' e^{\lambda(r)} - 8f_{\mathcal{G}} \mathcal{G}'' - 4f_{\mathcal{G}} \mathcal{G}' e^{\lambda(r)} \lambda' + 12f_{\mathcal{G}} \mathcal{G}' \lambda' \\ &- 12f_{\mathcal{G}} \mathcal{G}' e^{\lambda(r)} \chi' + 36f_{\mathcal{G}} \mathcal{G}' \chi' + 8f_{\mathcal{G}} \mathcal{G} \mathcal{G}'^2 e^{\lambda(r)} \\ &\left. - 8f_{\mathcal{G}} \mathcal{G} \mathcal{G}'^2 + 3pr^2 e^{\lambda(r)} - \rho r^2 e^{\lambda(r)} \right). \end{aligned} \quad (18)$$

CKV deliver favorable results due to their ability to provide a more detailed and comprehensive understanding of the geometry of spacetime. These vectors play a crucial role in the analysis of space geometry, offering intricate insights and facilitating a more thorough exploration of the underlying structures and properties of the spacetime manifold. Previous work on these equations exhibit that *CKV* in manifold is helpful technique for determining the analytical solution of the *EMFE* and given as

$$\mathfrak{f}_\eta g_{cd} = \Phi g_{cd}, \quad (19)$$

where, we have taken $c, d=0$ to 3 that illustrate space-time to be four-dimensional and $\mathfrak{f}_\eta g_{cd}$ represents the Lie derivative of metric tensor with respect to a vector field η . Further, by employing Eqs. (9) and (19), *CKV* can be written as

$$\begin{aligned} \eta^0 &= L, \quad \eta^1 \chi^1 = \Phi, \quad \eta^1 = \frac{\Phi r}{2}, \\ \eta^1 \lambda' + 2\xi^1_1 &= \Phi. \end{aligned} \quad (20)$$

We derive expressions for physical quantities by solving the set of simultaneous equations mentioned above, resulting in the following expressions

$$e^\chi = H^2 r^2, \quad e^\lambda = \left(\frac{I}{\Phi} \right)^2, \quad \xi^i = W \delta_4^i + \left(\frac{r \Phi}{2} \right) \delta_1^i, \quad (21)$$

where, W, H and I are constant parameters. A linear function Φ is considered i.e. $\Phi = H + Jr$, where J be the constant parameter.

3 Relativistic models of $f(\mathcal{G})$ gravity

The analysis in this study is carried out by utilizing two distinct and effective models of $f(\mathcal{G})$ gravity. The specifics are provided in upcoming sub-sections:

3.1 Model 1

We begin with the logarithmic model as described in [27, 29, 46]

$$f(\mathcal{G}) = \alpha \mathcal{G}^n + \beta \mathcal{G} \text{Log}(\mathcal{G}), \quad (22)$$

with constant parameters α and β . By employing Eqs. (14) – (16), Eqs. (21) and, (22), we obtain the expressions for effective energy density and pressure as

$$\begin{aligned} \rho^{eff} = \frac{1}{4r^{12}I^{10}s_1^n} & \left(4Br^{12}s_1^3I^{10} + \alpha 2^{3n+2}r^{12}s_1^3I^{10}s_{11}^n \right. \\ & + 3pr^{12}s_1^3I^{10} + 3\rho r^{12}s_1^3I^{10} + 32\beta r^9s_1^4I^6J \log(s_{11}) \\ & - 48r^9s_1^4s_9I^6J + 2r^9s_1^3s_{10}I^6 + 24r^5s_1s_3^2s_7I^4J(rJ + H) \\ & - 8r^5s_0s_3^2s_7I^6J - 32r^5s_0^2s_3s_7I^4J - 72r^4s_1s_3^2s_7I^4(rJ + H)^2 \\ & - 48r^4s_1s_2s_3s_7I^4(rJ + H)^2 - 64 \left(3r^4s_1s_2s_3s_7I^4 + 4s_3^2s_8J \right) \\ & \times \left(I^2 - (rJ + H)^2 \right) + 24r^4s_1s_3^2s_7I^6 + 48r^4s_1s_2s_3s_7I^6 \\ & \left. - 64s_3^2s_8J(rJ + H)^2 + 64s_3^2s_8I^2J \right), \quad (23) \end{aligned}$$

$$\begin{aligned} p^{eff} = \frac{1}{4r^{12}s_1^3I^{10}} & \left(-4Br^{12}s_1^3I^{10} + \alpha 2^{3n+2}r^{12}s_1^3I^{10}s_{11}^n \right. \\ & + pr^{12}s_1^3I^{10} + \rho r^{12}s_1^3I^{10} + 32\beta r^9s_1^4I^6J \log(s_{11}) \\ & - 16r^9s_1^4s_9I^6J + 2r^9s_1^3s_{10}I^6 - 24r^5s_1s_3^2s_7I^4J(rJ + H) \\ & + 8r^5s_0s_3^2s_7I^6J + 72r^4s_1s_3^2s_7I^4(rJ + H)^2 \\ & + 48r^4s_1s_2s_3s_7I^4(rJ + H)^2 + 32r^4s_1s_3^2s_7I^4 \\ & \times \left(I^2 - 3(rJ + H)^2 \right) - 24r^4s_1s_3^2s_7I^6 \\ & - 48r^4s_1s_2s_3s_7I^6 \\ & \left. + 64s_3^2s_8J(rJ + H)^2 - 64s_3^2s_8I^2J \right), \quad (24) \end{aligned}$$

where all expressions of s_i are mentioned in Appendix.

3.2 Model 2

In this study, we select another model to analyze the compact objects with conformal motion as presented in [51] and [48]

$$f(\mathcal{G}) = \xi \mathcal{G}^\gamma (\eta \mathcal{G}^\psi + 1), \quad (25)$$

where ξ , γ , η and ψ are arbitrary parameters. It is worthwhile to mention here that these are really important parameters as their values will help us in obtaining the physically realistic values of energy density and pressure. Now manipulating Eqs. (14) – (16), Eqs. (21), and (25), we attain following expression for effective density (ρ^{eff}) and effective pressure

$$(p^{eff})$$

$$\begin{aligned} \rho^{eff} = \frac{-1}{4r^{12}t_1^2t_3^4I^{10}(rJ + H)^3} & \left(-r^{12}t_3^4t_1^2I^{10}n \right. \\ & \times (4B + 3(p + \rho))(rJ + H)^3 \\ & + 3\eta\xi r^{12}t_3^4I^{10}2^{3\gamma+3\psi+1}(\gamma + \psi - 1)(rJ + H)^3 \\ & \times t_1^{\gamma+\psi+2} + 8^{\gamma+2}\xi r^6t_2^2t_7I^8t_1^{\gamma+3}(rJ + H) \\ & - 38^{\gamma+1}\xi r t_2t_3^4t_6J^2t_1^{\gamma}(rJ + H)^2(t_2(2rJ + H) \\ & \times (3r^2J^2 + 6rHJ + 3H^2 - I^2) \\ & + 2t_4(rJ + H)(r^2J^2 + 2rHJ + H^2 - I^2)) \\ & + 2^{3\gamma+1}\xi r^3t_3I^6t_1^{\gamma+2} \\ & \times (3(\gamma - 1)r^9t_3^3I^4(rJ + H)^3 - 32t_2^2t_7J) \\ & + 8^{\gamma+2}\xi t_2t_3^2Jt_1^{\gamma+1} \\ & \times (rJ + H)(r^2J^2 + 2rHJ + H^2 - I^2) \\ & \left. \times (3r^4t_3t_4t_6I^4(rJ + H) - 4t_2t_7J) \right), \quad (26) \end{aligned}$$

$$\begin{aligned} p^{eff} = \frac{-1}{4r^{11}t_1^2t_3^4I^{10}(rJ + H)^3} & \left(r^{11}t_3^4t_1^2I^{10}(4B - p - \rho)(rJ + H)^3 \right. \\ & + \eta\xi r^{11}t_3^4I^{10}2^{3\gamma+3\psi+1}(\gamma + \psi - 1) \\ & \times (rJ + H)^3t_1^{\gamma+\psi+2} \\ & - 8^{\gamma+2}\xi r^5t_2^2t_7I^8t_1^{\gamma+3}(rJ + H) \\ & - 8^{\gamma+1}\xi t_2t_3^4t_6J^2t_1^{\gamma}(rJ + H)^2(t_2(2rJ + H) \\ & \times (3r^2J^2 + 6rHJ + 3H^2 - I^2)) \\ & - 6t_4(rJ + H) \\ & \times (r^2J^2 + 2rHJ + H^2 - I^2)) \\ & + 2^{3\gamma+1}\xi r^2t_3I^6t_1^{\gamma+2}((\gamma - 1) \\ & \left. r^9t_3^3I^4(rJ + H)^3 + 32t_2^2t_7J \right), \quad (27) \end{aligned}$$

where, all expressions of t_i are mentioned in Appendix.

4 Matching with Bardeen geometry

Bardeen model is used to determine the solution and given by the following expression

$$ds^2 = L(r)^{-1}dr^2 + r^2d\theta^2 + r^2\sin^2\theta d^2 - L(r)dt^2, \quad (28)$$

where,

$$L(r) = 1 - \frac{2Mr^2}{(q^2 + r^2)^{\frac{3}{2}}}, \quad (29)$$

where M is the mass and this equation can be re-written as

$$L(r) = 1 - \frac{2M}{r} + \frac{3Mq^2}{r^3} + O\left(\frac{1}{r^5}\right). \quad (30)$$

In Eq. (30), the presence of the term involving the fraction r^3 sets Bardeen's model apart from the Reissner-Nordstrom solution. In our study, we adopt the expression for $L(r)$ as $L(r) = 1 - \frac{2M}{r} + \frac{3Mq^2}{r^3}$. To analyze certain attributes, we conduct a comparison between the exterior and interior configurations at the boundary ($r = R_b$) of the stars. In order to determine the values of e^χ and e^λ at this boundary, we utilize continuity conditions and results obtained from Eq. (21). This process leads us to the following matching constraints

$$1 - \frac{2M}{r} + \frac{3Mq^2}{r^3} = H^2 r^2, \quad (31)$$

$$\left(1 - \frac{2M}{r} + \frac{3Mq^2}{r^3}\right)^{-1} = \frac{I^2}{(H + Jr)^2}, \quad (32)$$

$$\frac{\partial g_{tt}^-}{\partial r} = \frac{\partial g_{tt}^+}{\partial r}, \quad (33)$$

here, $(-)$ and $(+)$ represents the interior and exterior solution respectively. Now for the further analysis, we assume $q^2 = \frac{gr^5}{gr+1}$ [45, 49]. Solving the Eqs. (31)–(33), we have the following expressions of constant parameters

$$H = -\sqrt{\frac{R_b(1+gR_b) - 2M(1+gR_b) + 3MgkR_b^3}{R_b^3 + gR_b^4}}, \quad (34)$$

$$I = -\frac{\sqrt{-2M+R_b-2qMR_b+gR_b^2+3gkMR_b^3} - JR_b^{\frac{5}{2}}\sqrt{1+gR_b}}{-R_b\sqrt{-2M+R_b-2qMR_b+gR_b^2+3gkMR_b^3}}, \quad (35)$$

$$J = -\frac{2\sqrt{1+gR_b}(R_b+gR_b^2-2M-2MgR_b+3MgkR_b^3)^{\frac{3}{2}}}{R_b^{\frac{5}{2}}(2R_b(1+gR_b)^2-6M-12MgR_b-6Mg^2R_b^2+3Mg^2kR_b^3)}. \quad (36)$$

These parameters play a major role in defining the behavior of a charged compact star, as they provide vital details about its charge distribution, geometry and the interaction of electromagnetic forces and gravity. Accurate determination of these parameters is essential for understanding the characteristics, stability and observational properties of charged compact stars.

5 Physical analysis

In this section, we demonstrate the detailed analysis of energy density, pressure distribution, EoS parameter, energy conditions, equilibrium conditions, and adiabatic parameter for the physical validity of stellar structure. We fix the constants $\alpha = 0.1$ and $\beta = 0.01$ for model 1 and the information about the rest of the constants is provided in Table 1. Moreover, the constants $\eta = 1.2$ and $\psi = 1.4$ are fixed for model 2 and the assumed values of the rest of all other constants are listed in the Table 2. The analysis is carried out by selecting the stars

PSR J1614 – 2230, PSR J1930 + 327, Cen X – 3 and Vela X – 1 with radius at least 9.

5.1 Profile of energy density and pressure distribution

The behavior of ρ^{eff} and p^{eff} in the context of the $f(\mathcal{G})$ theory of gravity exhibits credible characteristics. As depicted in Figs. 1 and 2, both ρ^{eff} and p^{eff} demonstrate a consistent pattern of decreasing values while remaining positive. Notably, as we approach the boundary of the star at $r = R_b$, the pressure approaches zero. The concave up graphical representations of ρ^{eff} and p^{eff} is a consequence of both conformal motion and the presence of electric charge within the system. We further analyze the gradients of energy density ($\frac{d\rho^{eff}}{dr}$) and pressure ($\frac{dp^{eff}}{dr}$) for both models, and their graphical representations can be found in Figs. 3 and 4, respectively. These aligns with physical expectations, notably their negative behavior, further affirming their physical acceptability. It may be noted that though the analysis is done for four stars, however, the graphical behavior in Figs. 1, 2, 3 and 4 is shown only for *PSR J1614 – 2230*. The other three stars exhibit the similar behavior of energy density and pressure profiles for both $f(\mathcal{G})$ models.

5.2 The energy conditions

In GR, the energy conditions (*ECs*) are essential in demonstrating the stability of the compact stars. Numerous researchers have presented the splendid characteristics of *ECs*. For a charged compact star to be considered physically viable, it must satisfy the *ECs*, ensuring that the energy density and pressures associated with the star's matter distribution meet certain criteria and do not violate fundamental principles of physics. Such conditions are null energy conditions (NEC), the weak energy condition (WEC), the strong energy condition (SEC) and the dominant energy condition (DEC). The *ECs* are provided by the following expressions

- Null energy conditions

$$\rho^{eff} + p^{eff} \geq 0, \quad \rho^{eff} + \frac{q^2}{4\pi r^4} \geq 0. \quad (37)$$

- Weak energy condition

$$\rho + \frac{q^2}{8\pi r^4} \geq 0, \quad \rho + p \geq 0, \quad \rho + p + \frac{q^2}{4\pi r^4} \geq 0. \quad (38)$$

- Strong energy conditions

$$\rho^{eff} + p^{eff} \geq 0, \quad \rho^{eff} + 3p^{eff} + \frac{q^2}{4\pi r^4} \geq 0. \quad (39)$$

Table 1 Values of unknown parameters for Model-I

Parameter	Stars	<i>PSR J1614 – 2230</i>	<i>PSR J1903 + 327</i>	<i>Vela X – 1</i>	<i>Cen X – 3</i>
n = 1.5	$M(M_{\odot})$	1.97	1.667	1.77	1.49
	R	10.30	9.82	9.99	9.61
	k	3.9	3.9	3.9	3.9
	H	– 1.63546	– 1.53397	– 1.56966	– 1.46317
	I	– 0.135973	– 0.142638	– 0.140204	– 0.145769
	J	– 0.0635965	– 0.0625936	– 0.0629489	– 0.0610304
n = 1.55	$M(M_{\odot})$	1.97	1.667	1.77	1.49
	R	10.30	9.82	9.99	9.61
	k	4	4	4	4
	H	– 1.65626	– 1.55347	– 1.58961	– 1.48176
	I	– 0.135972	– 0.142636	– 0.140202	– 0.145767
	J	– 0.0644034	– 0.0633865	– 0.0637468	– 0.0618025
n = 1.6	$M(M_{\odot})$	1.97	1.667	1.77	1.49
	R	10.30	9.82	9.99	9.61
	k	4.1	4.1	4.1	4.1
	H	– 1.67681	– 1.57273	– 1.60933	– 1.532
	I	– 0.135971	– 0.142634	– 0.140201	– 0.145762
	J	– 0.0652002	– 0.0641696	– 0.0645348	– 0.0638895
n = 1.65	$M(M_{\odot})$	1.97	1.667	1.77	1.49
	R	10.30	9.82	9.99	9.61
	k	4.2	4.2	4.2	4.2
	H	– 1.6971	– 1.59176	– 1.6288	– 1.55052
	I	– 0.13597	– 0.142633	– 0.140199	– 0.14576
	J	– 0.0659874	– 0.0649432	– 0.0653133	– 0.064659
n = 1.7	$M(M_{\odot})$	1.97	1.667	1.77	1.49
	R	10.30	9.82	9.99	9.61
	k	4.3	4.3	4.3	4.3
	H	– 1.71716	– 1.61056	– 1.64804	– 1.56883
	I	– 0.135969	– 0.142631	– 0.140198	– 0.145758
	J	– 0.0667654	– 0.0657078	– 0.0660826	– 0.0654196
n = 1.75	$M(M_{\odot})$	1.97	1.667	1.77	1.49
	R	10.30	9.82	9.99	9.61
	k	4.4	4.4	4.4	4.4
	H	– 1.73698	– 1.62914	– 1.66706	– 1.58692
	I	– 0.135968	– 0.14263	– 0.140196	– 0.145756
	J	– 0.0675344	– 0.0664635	– 0.0668431	– 0.0661713
n = 1.8	$M(M_{\odot})$	1.97	1.667	1.77	1.49
	R	10.30	9.82	9.99	9.61
	k	4.5	4.5	4.5	4.5
	H	– 1.75658	– 1.64751	– 1.68586	– 1.60481
	I	– 0.135967	– 0.142628	– 0.140195	– 0.145755
	J	– 0.0682947	– 0.0672108	– 0.067595	– 0.0669147

Table 2 Values of unknown parameters for Model-II

Parameter	Stars	<i>PSR J1614 – 2230</i>	<i>PSR J1903 + 327</i>	<i>Vela X – 1</i>	<i>Cen X – 3</i>
$\xi = 0.1$	$M(M_\odot)$	1.97	1.667	1.77	1.49
	R	10.30	9.82	9.99	9.61
	γ	0.01	0.01	0.01	0.01
	H	– 1.63546	– 1.53397	– 1.56966	– 1.46317
	I	– 0.135973	– 0.142638	– 0.140204	– 0.145769
	J	– 0.0635965	– 0.0625936	– 0.0629489	– 0.0610304
$\xi = 0.2$	$M(M_\odot)$	1.97	1.667	1.77	1.49
	R	10.30	9.82	9.99	9.61
	γ	0.02	0.02	0.02	0.02
	H	– 1.63546	– 1.53397	– 1.56966	– 1.46317
	I	– 0.135973	– 0.142638	– 0.140204	– 0.145769
	J	– 0.0635965	– 0.0625936	– 0.0629489	– 0.0610304
$\xi = 0.3$	$M(M_\odot)$	1.97	1.667	1.77	1.49
	R	10.30	9.82	9.99	9.61
	γ	0.04	0.04	0.04	0.04
	H	– 1.63546	– 1.53397	– 1.56966	– 1.46317
	I	– 0.135973	– 0.142638	– 0.140204	– 0.145769
	J	– 0.0635965	– 0.0625936	– 0.0629489	– 0.0610304
$\xi = 0.4$	$M(M_\odot)$	1.97	1.667	1.77	1.49
	R	10.30	9.82	9.99	9.61
	γ	0.07	0.07	0.07	0.07
	H	– 1.64589	– 1.54375	– 1.57967	– 1.47249
	I	– 0.135973	– 0.142637	– 0.140203	– 0.145768
	J	– 0.0640012	– 0.0629913	– 0.0633491	– 0.0614177
$\xi = 0.5$	$M(M_\odot)$	1.97	1.667	1.77	1.49
	R	10.30	9.82	9.99	9.61
	γ	0.09	0.09	0.09	0.09
	H	– 1.65626	– 1.55347	– 1.58961	– 1.48176
	I	– 0.135972	– 0.142636	– 0.140202	– 0.145767
	J	– 0.0644034	– 0.0633865	– 0.0637468	– 0.0618025
$\xi = 0.6$	$M(M_\odot)$	1.97	1.667	1.77	1.49
	R	10.30	9.82	9.99	9.61
	γ	0.1	0.1	0.1	0.1
	H	– 1.67681	– 1.57273	– 1.60933	– 1.50012
	I	– 0.135971	– 0.142634	– 0.140201	– 0.145765
	J	– 0.0652002	– 0.0641696	– 0.0645348	– 0.0625651
$\xi = 0.7$	$M(M_\odot)$	1.97	1.667	1.77	1.49
	R	10.30	9.82	9.99	9.61
	γ	0.12	0.12	0.12	0.12
	H	– 1.68698	– 1.58227	– 1.61909	– 1.50921
	I	– 0.13597	– 0.142634	– 0.1402	– 0.145764
	J	– 0.065595	– 0.0645576	– 0.0649252	– 0.062943

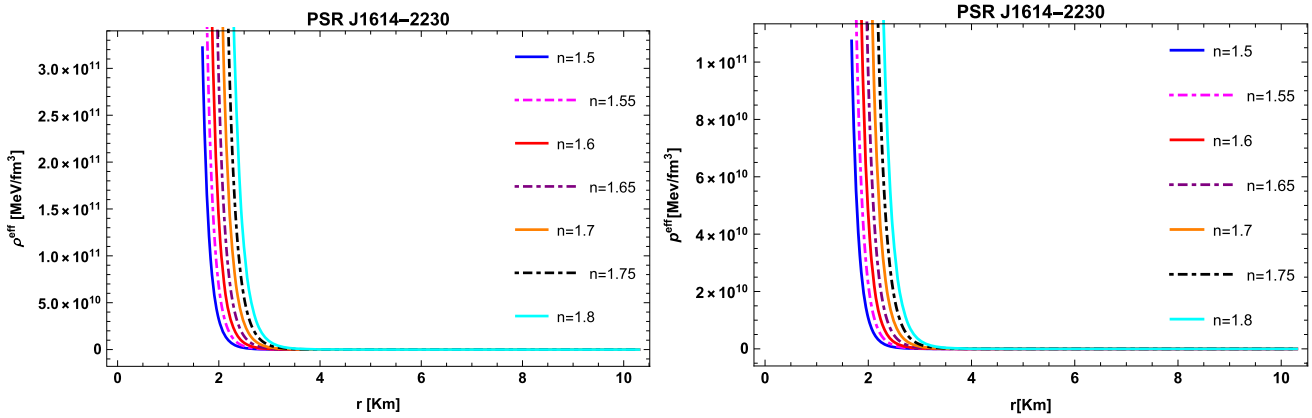


Fig. 1 Behavior of energy density ρ^{eff} and pressure p^{eff} for Model-1

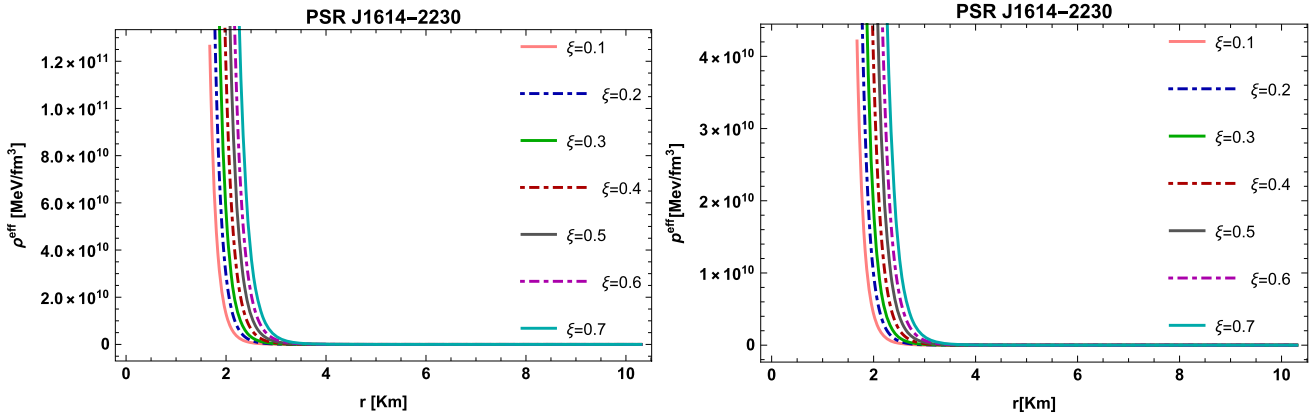


Fig. 2 Behavior of energy density ρ^{eff} and pressure p^{eff} for Model-2

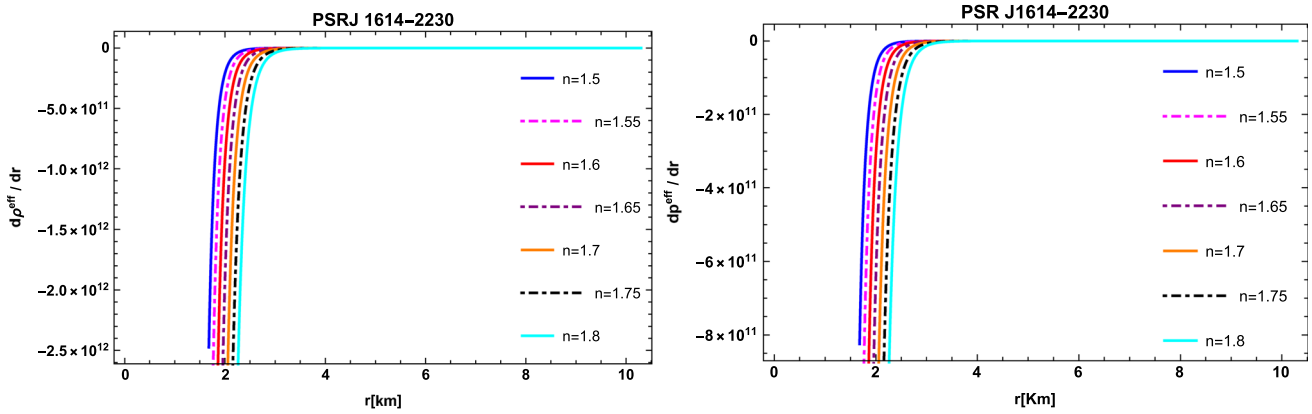


Fig. 3 Behavior of derivative of ρ^{eff} and pressure p^{eff} for Model-1

It can be noticed from Figs. 5 and 6 that all the ECs are satisfied for both models for *PSR J1614 – 2230*, which means that our considered models are viable. It is worthwhile to mention here that the graphical behavior of ECs for other three stars is same as *PSR J1614 – 2230* and it is not provided just to avoid the repetition of similar figures.

5.3 Equilibrium condition

Here, we discuss the equilibrium condition in the scenario of Bardeen geometry with conformal motions for the existing charged stellar structure. The Tolman Oppenheimer Volkof (*TOV*) equation is very useful to examine the equilibrium condition for stellar structure. The *TOV* equation in pres-

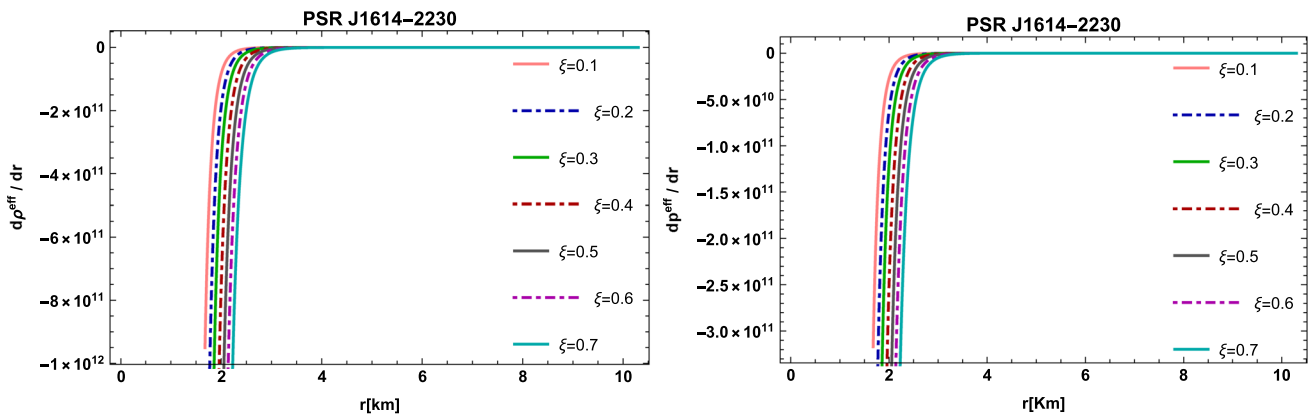


Fig. 4 Behavior of derivative of ρ^{eff} and pressure p^{eff} for Model-2

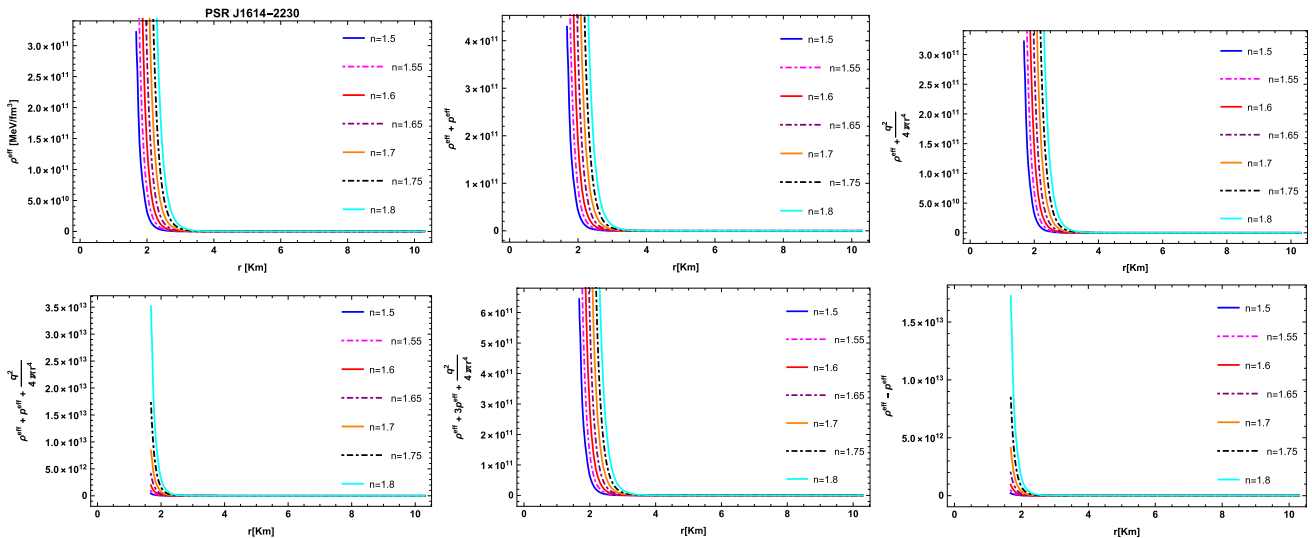


Fig. 5 Behavior of EC for star $PSR\ J1614 - 2230$ for Model-I

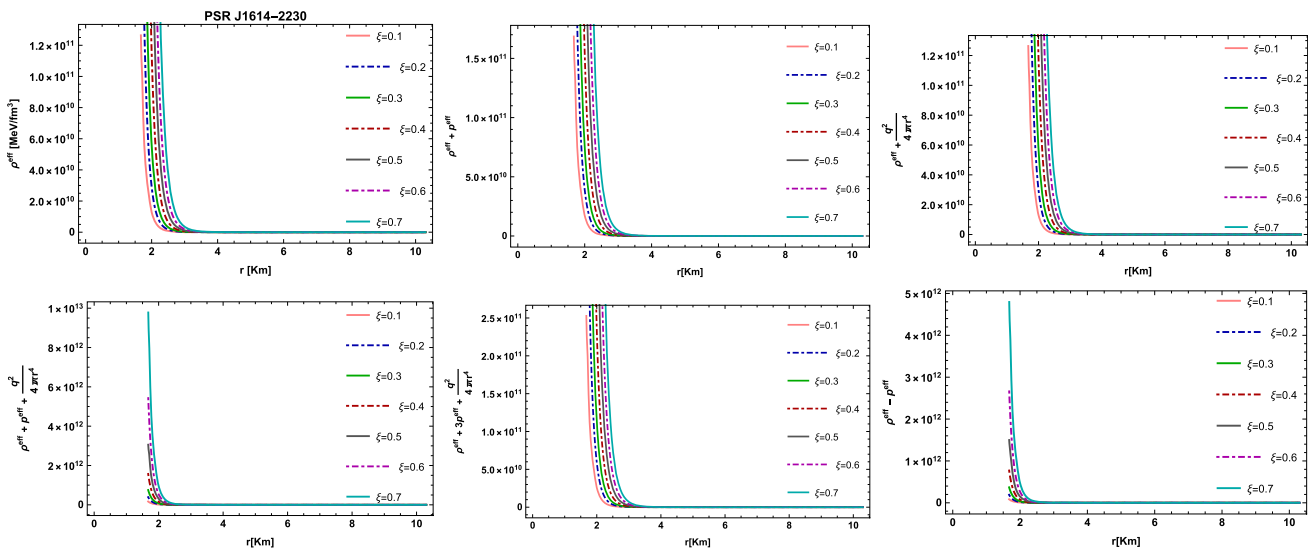


Fig. 6 Behavior of EC of star $PSR\ J1614 - 2230$ for Model-II

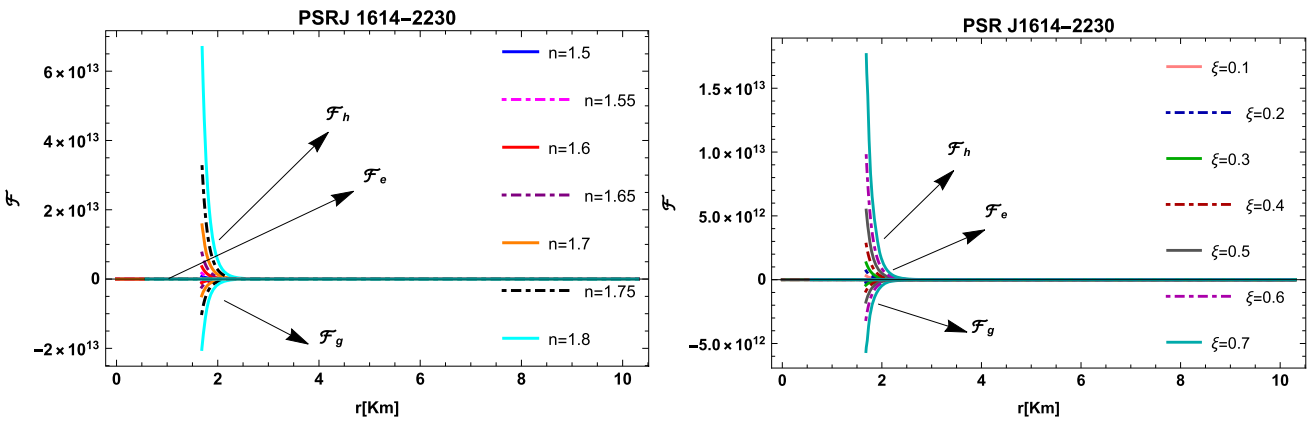


Fig. 7 Behavior of \mathcal{F}_h , \mathcal{F}_g and \mathcal{F}_e for Model-I (Left plot) and Model-II (Right plot)

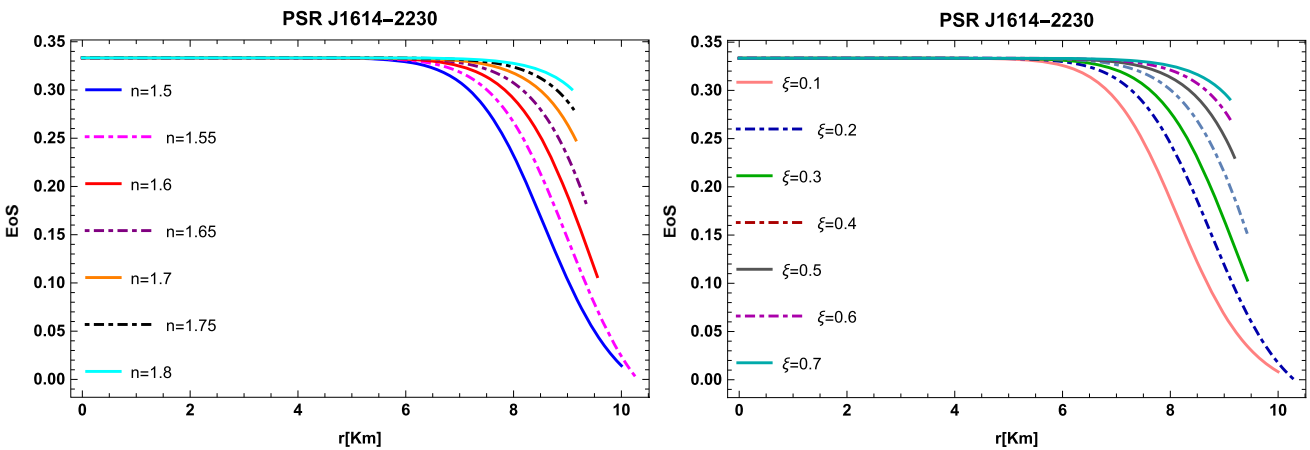


Fig. 8 Evolution of EoS parameter w for Model-I (Left plot) and Model-II (Right plot)

ences of charged isotropic distribution are given as

$$-\frac{\chi'}{2}(\rho^{eff} + p^{eff}) + \sigma(r)E(r)e^{\frac{\lambda(r)}{2}} - \frac{dp^{eff}}{dr} = 0. \quad (40)$$

This equation can also be expressed as

$$\mathcal{F}_g + \mathcal{F}_e + \mathcal{F}_h = 0. \quad (41)$$

- Gravitational force

$$\mathcal{F}_g = -\frac{\chi'}{2}(\rho^{eff} + p^{eff}). \quad (42)$$

- Electric force

$$\mathcal{F}_e = \sigma(r)E(r)e^{\frac{\lambda(r)}{2}}. \quad (43)$$

- Hydrostatic force

$$\mathcal{F}_h = -\frac{dp^{eff}}{dr}. \quad (44)$$

Figure 7 exhibits that the equilibrium condition is fulfilled for the presented $f(\mathcal{G})$ models for PSR J1614-2230. The equilibrium condition is also satisfied for the other three compact stars (though not shown here).

5.4 Equation of state parameter

In this sub-section, we conduct an investigation of EoS parameters, which are represented by the following expression

$$w = \frac{p^{eff}}{\rho^{eff}}. \quad (45)$$

The graphical behaviors of w of both models for PSR J1614-2230 are shown in Fig. 8, which indicate that the EoS of the selected $f(\mathcal{G})$ models falls within a range that corresponds to normal matter, and ensuring the stability of the stars. Further, the high degree of compactness observed in these models suggests that they exhibit a dense and compact nature.

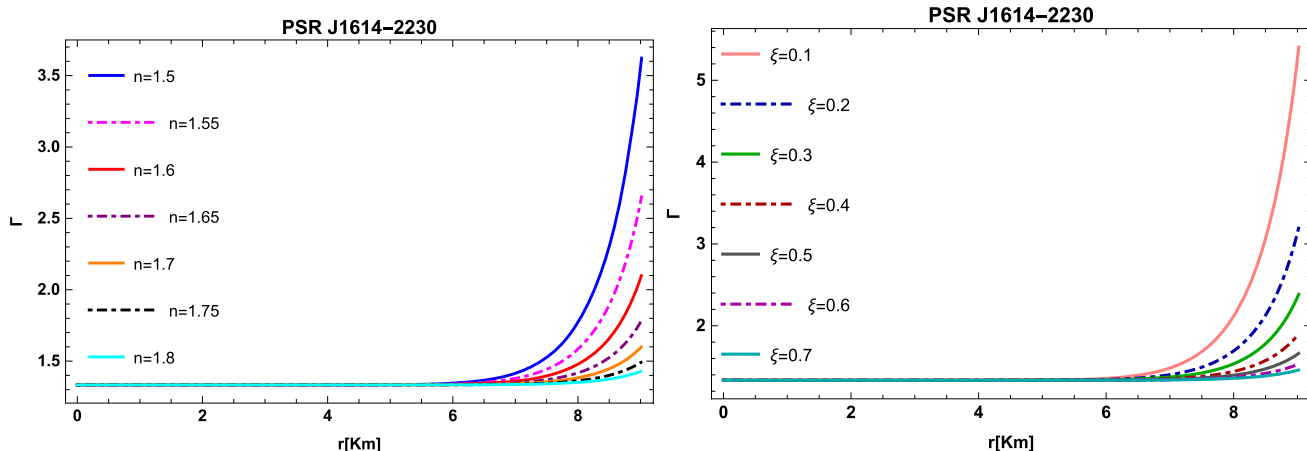


Fig. 9 Graphical illustration of adiabatic index for Model-I (Left plot) and Model-II (Right plot)

5.5 Casualty condition and adiabatic index

We have checked the casualty condition according to Herrera's cracking concept, which is defined as

$$v^2 = \frac{dp^{eff}}{d\rho^{eff}}. \quad (46)$$

This sound speed v^2 lies between the limits 0 and 1, which demonstrates the consistency of our $f(\mathcal{G})$ models. Chandarshekhar [50] introduced criteria for insatiability based on the adiabatic parameter, where it serves as an effective barrier between a large gravitational field and a small nuclear force. The formula for this is given as

$$\Gamma = \left(1 + \frac{\rho^{eff}}{p^{eff}} \frac{dp^{eff}}{d\rho^{eff}} \right). \quad (47)$$

According to Chandarshekhar's criteria, the adiabatic index should be greater than $4/3$. Figure 9 shows that the our both models are stable.

6 Conclusion

In current study, we select the Bardeen black hole geometry with conformal motion and apply the matching condition to two different models of modified $f(\mathcal{G})$ gravity, namely $f(\mathcal{G}) = \alpha\mathcal{G}^n + \beta\mathcal{G}\text{Log}(\mathcal{G})$ and $f(\mathcal{G}) = \xi G^\gamma (\eta G^\psi + 1)$ in the presence of an electric charge with isotropic energy momentum tensor. The analysis is tabulated for four different stars: *PSRJ1614 – 2230*, *PSRJ1930 + 327*, *Cen X – 3*, and *Vela X – 1*. It may be noted that the graphical behavior is shown only for *PSR J1614 – 2230*. The other three stars exhibit the similar behavior for both $f(\mathcal{G})$ models as that of *PSR J1614 – 2230*. To achieve feasible results, we analyze model 1 for different values of n and model 2 for different values of ξ . The final outcomes of our work are as follows:

- The solutions found with conformal symmetries for the metric potentials are finite, bounded and singularity free across the star and also at the boundary i.e. $r = R_b$. The analysis of ρ^{eff} and p^{eff} are shown in Figs. 1 to 2. The negative behavior of derivatives $d\rho^{eff}/dr$ and dp^{eff}/dr show that they are acceptable for the present study as shown in Figs. 3 and 4.
- We also study the *ECs* such that NEC, WEC, DEC, and SEC for both $f(\mathcal{G})$ models. It can be noticed from Figs. 5 and 6 that both models satisfy all of the given *ECs* under conformal motion, which means that our considered models are viable.
- The equilibrium condition for the current charged stellar configuration utilizing *TOV* equations in the presence of Bardeen geometry along with CKV is illustrated in Fig. 7. It can be seen that the equilibrium condition is satisfied for the presented $f(\mathcal{G})$ models, which means that our both models are valid and reliable in the presence of electric charge.
- It can be observed from Fig. 8 that both models satisfy the EoS parameter which implies that the stars are stable. Moreover, the graphical analysis of adiabatic index for both $f(\mathcal{G})$ models can be seen in Fig. 9, which means that our considered stars are stable.

In nutshell, we are able to create an effective and stable stellar configuration in the existence of charge by employing two different $f(\mathcal{G})$ gravity models along with Bardeen black hole geometry with conformal motion. It is important to mention here that the results of our manuscript agree with already reported work in general relativity [49]. It is interesting to notice that modified $f(\mathcal{G})$ theory of gravity supports more massive stars (upto a solar mass 1.97 and radius 10.30km) as compared to general relativity [49].

Acknowledgements Adnan Malik acknowledges the Grant No. YS304023912 to support his Postdoctoral Fellowship at Zhejiang Normal University, China. M. Farasat Shamir is thankful to Prof. Alex Clark for the hospitality and encouragement during the stay at QMUL where this work was completed.

Data Availability Statement This manuscript has no associated data or the data will not be deposited. [Authors' comment: This is a theoretical study and no experimental data.]

Declarations

Conflict of interest The authors have declared that they have no interest of conflict.

Open Access This article is licensed under a Creative Commons Attribution 4.0 International License, which permits use, sharing, adaptation, distribution and reproduction in any medium or format, as long as you give appropriate credit to the original author(s) and the source, provide a link to the Creative Commons licence, and indicate if changes were made. The images or other third party material in this article are included in the article's Creative Commons licence, unless indicated otherwise in a credit line to the material. If material is not included in the article's Creative Commons licence and your intended use is not permitted by statutory regulation or exceeds the permitted use, you will need to obtain permission directly from the copyright holder. To view a copy of this licence, visit <http://creativecommons.org/licenses/by/4.0/>.

Funded by SCOAP³. SCOAP³ supports the goals of the International Year of Basic Sciences for Sustainable Development.

Appendix

Where all s_i and t_i used in Sect. 3 are given as

$$\begin{aligned}
 s_0 &= 3r^2J^2 + 6rHJ + 3H^2 - I^2 \\
 s_1 &= (rJ + H)(3r^2J^2 + 6rHJ + 3H^2 - I^2) \\
 s_2 &= (rJ + 2H)(3rHJ + 3H^2 - I^2) \\
 s_3 &= 9r^2HJ^2 + 18rH^2J - 2rI^2J + 9H^3 - 3HI^2 \\
 s_4 &= \alpha(6H(3r^5J^5 - rI^4J) - 72H^3(r^3J^3 - rI^2J) \\
 &\quad + 6H^4(5I^2 - 33r^2J^2) - 2r^2I^2J^2(3r^2J^2 + I^2) \\
 &\quad + H^2(27r^4J^4 + 48r^2I^2J^2 - 5I^4) - 162rH^5J - 45H^6) \\
 s_5 &= \alpha(18H^3(3r^3J^3 + 2rI^2J) + 18H^4(I^2 - 3r^2J^2) \\
 &\quad - r^2I^2J^2(9r^2J^2 + I^2) + 3H(9r^5J^5 - 6r^3I^2J^3 - rI^4J) \\
 &\quad + H^2(81r^4J^4 + 9r^2I^2J^2 - 3I^4) - 81rH^5J - 27H^6) \\
 s_6 &= 8J(rJ + H)(162H^5(25r^3J^3 - 3rI^2J) \\
 &\quad - 81H^6(I^2 - 27r^2J^2) \\
 &\quad + 27H^4(165r^4J^4 - 44r^2I^2J^2 + I^4) \\
 &\quad + 108rH^3J(27r^4J^4 - 14r^2I^2J^2 + I^4) \\
 &\quad - 2r^2I^2J^2(27r^4J^4 - 12r^2I^2J^2 + I^4) \\
 &\quad + 6H(27r^7J^7 - 63r^5I^2J^5 \\
 &\quad + 17r^3I^4J^3 - rI^6J) - 3H^2(-351r^6J^6 + 351r^4I^2J^4 \\
 &\quad - 53r^2I^4J^2 + I^6) + 648rH^7J + 81H^8)
 \end{aligned}$$

$$\begin{aligned}
 s_7 &= \alpha(-8^n)n^2r^3I^4\left(\frac{s_1J}{r^3I^4}\right)^n + \alpha8^nr^3I^4\left(\frac{s_1J}{r^3I^4}\right)^n - 8\beta s_1J \\
 s_8 &= \alpha8^nn^3r^3s_3^2I^4\left(\frac{s_1J}{r^3I^4}\right)^n + 38^nn^2r^3s_4I^4\left(\frac{s_1J}{r^3I^4}\right)^n \\
 &\quad - 2^{3n+1}nr^3s_5I^4\left(\frac{s_1J}{r^3I^4}\right)^n + \beta s_6 \\
 s_9 &= \beta + \alpha8^{n-1}n\left(\frac{s_1J}{r^3I^4}\right)^{n-1} + \beta \log\left(\frac{8s_1J}{r^3I^4}\right) \\
 s_{10} &= \alpha8^nr^3I^4\left(\frac{s_1J}{r^3I^4}\right)^n + 8\beta s_1J \log\left(\frac{8s_1J}{r^3I^4}\right) \\
 s_{11} &= \frac{s_1J}{r^3I^4} \\
 t_1 &= \frac{J(rJ + H)(3r^2J^2 + 6rHJ + 3H^2 - I^2)}{r^3I^4} \\
 t_2 &= 9r^2HJ^2 + 18rH^2J - 2rI^2J + 9H^3 - 3HI^2 \\
 t_3 &= 3r^2J^2 + 6rHJ + 3H^2 - I^2 \\
 t_4 &= (rJ + 2H)(3rHJ + 3H^2 - I^2) \\
 t_5 &= 2rJ(rJ + H)(9rHJ + 9H^2 - I^2) \\
 t_6 &= \gamma^2\left(\eta 8^\psi t_1^\psi + 1\right) + \gamma\left(\eta 8^\psi(2\psi - 1)t_1^\psi - 1\right) \\
 &\quad + \eta 8^\psi(\psi - 1)\psi t_1^\psi \\
 t_7 &= 4t_2t_3t_6(rJ + H) + \eta t_2^2 8^\psi \psi \\
 &\quad \left(\gamma^2 + \gamma(2\psi - 1) + (\psi - 1)\psi\right) t_1^\psi \\
 &\quad - (2 - \gamma)t_2^2 t_6 - t_5t_3t_6
 \end{aligned}$$

References

1. H.A. Buchdahl, Non-linear Lagrangians and cosmological theory. Mon. Not. R. Astron. Soc. **150**(1), 1–8 (1970)
2. S. Nojiri, S.D. Odintsov, Unified cosmic history in modified gravity: from $F(R)$ theory to Lorentz non-invariant models. Phys. Rep. **505**(2–4), 59–144 (2011)
3. S.A. Mardan et al., Spherically symmetric generating solutions in $f(R)$ theory. Eur. Phys. J. Plus **138**(9), 782 (2023)
4. M.F. Shamir, A. Malik, Bardeen compact stars in modified $f(R)$ gravity. Chin. J. Phys. **69**, 312–321 (2021)
5. S. Nojiri et al., Modified gravity theories on a nutshell: inflation, bounce and late-time evolution. Phys. Rep. **692**, 1–104 (2017)
6. Naz et al., Evolving embedded traversable wormholes in $f(R, G)$ gravity: a comparative study. Phys. Dark Univ. **42**, 101301 (2023)
7. S. Nojiri, S.D. Odintsov, Modified Gauss–Bonnet theory as gravitational alternative for dark energy. Phys. Lett. B **631**(1–2), 1–6 (2005)
8. Z. Yousaf et al., Stability of anisotropy pressure in self-gravitational systems in $f(G)$ gravity. Axioms **12**(3), 257 (2023)
9. M.F. Shamir et al., Relativistic Kröri–Barua compact stars in $f(R, T)$ gravity. Fortschr. Phys. **70**(12), 2200134 (2022)
10. T. Harko et al., $f(R, T)$ gravity. Phys. Rev. D **84**(2), 024020 (2011)
11. Bhar et al., Physical characteristics and maximum allowable mass of hybrid star in the context of $f(Q)$ gravity. Eur. Phys. J. C **83**, 646 (2023)
12. A. Malik et al., Investigation of traversable wormhole solutions in $f(R, \phi)$ gravity utilizing the Karmarkar condition. Eur. Phys. J. C **83**, 522 (2023)

13. A. Malik, Analysis of charged compact stars in modified $f(R, \phi)$ theory of gravity. *New Astron.* **93**, 101765 (2022)
14. A. Malik et al., A study of charged stellar structure in modified $f(R, \phi, X)$ gravity. *Int J Geom. Methods Mod. Phys.* **19**(11), 2250180 (2022)
15. A. Malik et al., A study of cylindrically symmetric solutions in $f(R, \phi, X)$ theory of gravity. *Eur. Phys. J. C* **82**(2), 166 (2022)
16. K. Bamba et al., Dark energy cosmology: the equivalent description via different theoretical models and cosmography tests. *Astrophys. Space Sci.* **342**, 155–228 (2012)
17. G. Cognola et al., On the stability of a class of modified gravitational models. *Int. J. Theor. Phys.* **47**, 898–910 (2008)
18. C.G. Boehmer, F.S.N. Lobo, Stability of the Einstein static universe in modified Gauss–Bonnet gravity. *Phys. Rev. D* **79**(6), 067504 (2009)
19. J. Sadeghi et al., Cosmic acceleration and crossing of $w = -1$ in non-minimal modified Gauss–Bonnet gravity. *Phys. Lett. B* **679**(4), 302–305 (2009)
20. S. Nojiri et al., From inflation to dark energy in the non-minimal modified gravity. *Prog. Theor. Phys. Suppl.* **172**, 81–89 (2008)
21. D. Wang et al., Observational constraints on a logarithmic scalar field dark energy model and black hole mass evolution in the universe. *Eur. Phys. J. C* **83**(7), 670 (2023)
22. G. Cognola et al., String-inspired Gauss–Bonnet gravity reconstructed from the universe expansion history and yielding the transition from matter dominance to dark energy. *Phys. Rev. D* **75**(8), 086002 (2007)
23. J. Santos et al., Energy conditions and cosmic acceleration. *Phys. Rev. D* **75**(8), 083523 (2007)
24. M.K. Mak, T. Harko, Quark stars admitting a one-parameter group of conformal motions. *Int. J. Mod. Phys. D* **13**(01), 149–156 (2004)
25. M. Chaisi, S.D. Maharaj, Compact anisotropic spheres with prescribed energy density. *Gen. Relat. Gravit.* **37**, 1177–1189 (2005)
26. M. Kalam et al., Anisotropic strange star with de Sitter spacetime. *Eur. Phys. J. C* **72**, 1–7 (2012)
27. M. Ilyas, Charged compact stars in $f(G)$ gravity. *Eur. Phys. J. C* **78**(9), 757 (2018)
28. De-Felice, S. Tsujikawa, Construction of cosmologically viable $f(G)$ gravity models. *Phys. Lett. B* **675**(1), 1–8 (2009)
29. T. Naz, M.F. Shamir, Dynamical behavior of stellar structures in $f(G)$ gravity. *Theor. Math. Phys.* **205**(2), 1527–1545 (2020)
30. M.F. Shamir, T. Naz, Stellar structures in $f(G)$ gravity with Tolman–Kuchowicz spacetime. *Phys. Dark Univ.* **27**, 100472 (2020)
31. M.F. Shamir, T. Naz, Stellar structures in $f(G)$ gravity admitting Noether symmetries. *Phys. Lett. B* **806**, 135519 (2020)
32. Malik et al., Bardeen compact stars in modified $f(G)$ gravity. *Can. J. Phys.* **100**, 452–462 (2022)
33. L. Herrera et al., Anisotropic fluids and conformal motions in general relativity. *J. Math. Phys.* **25**(11), 3274–3278 (1984)
34. L. Herrera, J. Ponce de Leon, Anisotropic spheres admitting a one-parameter group of conformal motions. *J. Math. Phys.* **26**(8), 2018–2023 (1985)
35. L. Herrera, J. Ponce de Leon, Isotropic and anisotropic charged spheres admitting a one-parameter group of conformal motions. *J. Math. Phys.* **26**(9), 2302–2307 (1985)
36. R. Maartens, M.S. Maharaj, Conformally symmetric static fluid spheres. *J. Math. Phys.* **31**(1), 151–155 (1990)
37. P. Bhar et al., Possibility of higher-dimensional anisotropic compact star. *Eur. Phys. J. C* **75**(5), 190 (2015)
38. A.A. Usmani et al., Charged gravastars admitting conformal motion. *Phys. Lett. B* **701**(4), 388–392 (2011)
39. A. Das et al., Relativistic compact stars in $f(T)$ gravity admitting conformal motion. *Astrophys. Space Sci.* **358**(2), 36 (2015)
40. M. Zubair et al., Interior solutions of fluid sphere in $f(R, T)$ gravity admitting conformal killing vectors. *Astrophys. Space Sci.* **361**(7), 238 (2016)
41. D. Deb et al., Relativistic model for anisotropic strange stars. *Ann. Phys.* **387**, 239–252 (2017)
42. A.A. Coley, B. Tupper, Spherically symmetric spacetimes admitting inheriting conformal Killing vector fields. *Class. Quantum Gravity* **7**(12), 2195 (1990)
43. G. Abbas, M.R. Shahzad, Isotropic compact stars model in Rastall theory admitting conformal motion. *Astrophys. Space Sci.* **363**(12), 251 (2018)
44. J.W. Jape et al., Generalized compact star models with conformal symmetry. *Eur. Phys. J. C* **81**, 1–12 (2021)
45. M.F. Shamir, A. Rashid, Bardeen compact stars in modified $f(R)$ gravity with conformal motion. *Int. J. Geometr. Methods Mod. Phys.* **20**(02), 2350026 (2023)
46. H.J. Schmidt, Gauss–Bonnet Lagrangian $G \ln G$ and cosmological exact solutions. *Phys. Rev. D* **83**, 083513 (2011)
47. M.F. Shamir, Massive compact Bardeen stars with conformal motion. *Phys. Lett. B* **811**, 135927 (2020)
48. M. Ilyas, Charged compact stars in $f(G)$ gravity. *Eur. Phys. J. C* **78**(9), 757 (2018)
49. M.F. Shamir, G. Mustafa, Charged anisotropic Bardeen spheres admitting conformal motion. *Ann. Phys.* **418**, 168184 (2020)
50. S. Chandrasekhar, The dynamical instability of gaseous masses approaching the Schwarzschild limit in general relativity. *Phys. Rev. Lett.* **12**(4), 114 (1964)
51. K. Bamba et al., Finite-time future singularities in modified Gauss–Bonnet and $f(R, G)$ gravity and singularity avoidance. *Eur. Phys. J. C* **67**, 295–310 (2010)